Iodine-123-Metaiodobenzylguanidine Myocardial Imaging in Patients with Right Ventricular Pressure Overload

Takuya Morimitsu, Yoshiyuki Miyahara, Hiroki Sinboku, Satoshi Ikeda, Tatsuji Naito, Kyouji Nishijima and Masami Takao
The Second Department of Internal Medicine, Nagasaki University, School of Medicine, Nagasaki, Japan

Iodine-123-metaiodobenzylguanidine ([^{123}I]MIBG) has been used to evaluate the cardiac sympathetic nervous system, particularly that of the left heart. To clarify whether the right ventricular (RV) sympathetic neuronal function could be evaluated by [^{123}I]MIBG myocardial imaging, we applied the technique in patients with pulmonary hypertension that was associated with either chronic pulmonary diseases or pulmonary vascular diseases. **Methods:** All patients underwent right heart catheterization, and right heart hemodynamics were determined during a clinically stable state. SPECT was performed in the resting state 15 min (early imaging) and 4 hr (delayed imaging) postadministration of [^{123}I]MIBG. Seven regions of interest (ROI) were selected on the delayed short-axis images on the RV free wall, left ventricular (LV) free wall and interventricular septum (IVS). We calculated the IVS-to-LV uptake ratio from the scintillation counts of the ROI. Thallium-201 myocardial imaging was also performed within 1 wk after [^{123}I]MIBG imaging. **Results:** Images obtained with these techniques were analyzed for the RV-to-LV uptake ratio. The IVS-to-LV ratio on [^{123}I]MIBG correlated negatively and significantly with the mean pulmonary arterial pressure (PAm). The RV-to-LV uptake ratio on ^{201}Tl images correlated significantly with PAm. **Conclusion:** Our results suggest that the uptake ratio of [^{123}I]MIBG in the IVS is a useful index for evaluating the severity of pulmonary hypertension, and that chronic RV pressure overload contributes to disturbances of the cardiac sympathetic nervous system.

Key Words: pulmonary hypertension; cardiac sympathetic nervous system; interventricular septum; right ventricular hypertrophy; iodine-123-MIBG

J Nucl Med 1996; 37:1343–1346

Iodine-123-metaiodobenzylguanidine ([^{123}I]MIBG), an analog of norepinephrine (NE), is similar to NE with regard to its uptake, storage and release in sympathetic nerve endings. Like NE, ^{123}I also accumulates in the cardiac muscle through uptake into and release from NE storage vesicles of the sympathetic nerve endings. Iodine-123-MIBG is taken up into NE storage vesicles of the sympathetic nerve endings via intraneuronal accumulation [uptake-1 (Na^+-dependent) and extraneural accumulation, uptake-2 (passive diffusion)] and is released by exocytosis. Its accumulation is considered to reflect the activity of cardiac sympathetic neurons (*1–6*). Several reports have examined the relationship between [^{123}I]MIBG and a variety of diseases affecting the left heart, such as ischemic heart diseases, diabetes and cardiomyopathy. Relatively few studies, however, have examined the relationship between [^{123}I]MIBG and diseases that affect the right heart (*7–12*). In this study, SPECT was used to assess the relationship between chronic right ventricular (RV) pressure overload and cardiac sympathetic neuronal function in patients with chronic pulmonary diseases and pulmonary vascular diseases.

Received May 1, 1995; revision accepted Nov. 3, 1995.
For correspondence or reprints contact: Takuya Morimitsu, MD, Second Department of Internal Medicine, Nagasaki University, School of Medicine, 1-7-1 Sakamoto, Nagasaki 852, Japan.

METHODS

Patients

A total of 20 patients were studied, including eight patients with pulmonary thromboembolism, three with pulmonary emphysema, three with prior pulmonary tuberculosis, two with collagenosis lung in systemic lupus erythematosus, two with aortitis syndrome and two with diffuse panbronchiolitis. No patients had received any drugs that influence sympathetic neuronal function, such as reserpine. Patients suffering from hypertension, valvular diseases, ischemic heart diseases, cardiomyopathy and diabetes were excluded from the study.

After obtaining informed consent from all subjects, respiratory function tests and right heart catheterization were performed to evaluate right heart hemodynamics (Table 1).

Imaging Technique

Lugol solution (40 mg/day of iodure) was administered orally for 3 days both before and after scintigraphic examination. On the day of the examination, patients were instructed to fast until the last imaging session was complete at 4 hr. SPECT imaging was performed with the patient in the supine position, and images were obtained 15 min (early image) and 4 hr (delay image) after intravenous injection 111 MBq [^{123}I]MIBG into the antecubital vein. The SPECT instrument was equipped with three scintillation cameras and a high-resolution, low-energy, parallel-hole collimator connected to a computer system. SPECT images were acquired at an energy level of 159 keV, a window width of 20%, for 40 sec per direction, with the step angle set at 5° × 24 steps. Data were obtained for a 64 × 64-pixel matrix over 360°. Tomograms were reconstructed with a low-pass filter set at 8.1 cycles/pixel and a cutoff value of 0.25 Hz after processing the original image and a ramp image reconstruction filter. Thallium-201 SPECT scans of the cardiac muscles were performed within 1 wk after [^{123}I]MIBG myocardial SPECT imaging. Following intravenous injection of 111 MBq ^{201}Tl, tomographs were taken and reconstructed in a manner similar to that used for the [^{123}I]MIBG SPECT scans with the exception that the energy level was set at 75 keV for the ^{201}Tl scans.

Data Analysis

Axial cross-sectional images, short axial images, perpendicular major axial images and horizontal major axial images were produced for both the [^{123}I]MIBG and ^{201}Tl scans. The delayed images were used to examine the right ventricle and evaluate the level of hypertrophy using the short axial image of the ventricle's middle region. Furthermore, seven 6 × 6-pixel regions of interest (ROIs) each were set in three regions in the RV free wall, three in the left ventricular (LV) free wall and one in the interventricular septum (IVS) (Fig. 1). Scintillation counts of myocardial wall were determined (Fig. 2), and the RV-to-LV uptake ratio and the

TABLE 1
Hemodynamics, Pulmonary Function and Blood Gases

Sex (M:F)	10:10
Age (yr)	61.8 ± 2.5
PaO_2 (torr)	71.0 ± 2.2
$PaCO_2$ (torr)	37.6 ± 1.2
PAm (mmHg)	27.7 ± 2.5
PCWP (mmHg)	7.7 ± 0.7
CO (liter/min)	5.0 ± 0.3
CI (liter/min/m^2)	3.1 ± 0.2
% VC (%)	86.0 ± 7.0
FEV 1.0% (%)	61.8 ± 4.9
% DLCO (%)	63.9 ± 7.2

PAm = mean pulmonary arterial pressure; PCWP = mean pulmonary capillary wedge pressure; CO = cardiac output CI, cardiac index; % VC = % vital capacity; FEV 1.0% = % forced expiratory volume in 1 sec; % DLCO = % pulmonary diffusing capacity.

IVS-to-LV uptake ratio were calculated using the following equations:

$$\text{RV-to-LV upatke ratio (\%)} = \frac{(\text{ROI 1} + \text{ROI 2} + \text{ROI 3})}{(\text{ROI 5} + \text{ROI 6} + \text{ROI 7})} \times 100 \quad \text{Eq. 1}$$

$$\text{IVS-to-LV uptake ratio (\%)} = \frac{\text{ROI 4}}{(\text{ROI 5} + \text{ROI 6} + \text{ROI 7})} \times 100 \quad \text{Eq. 2}$$

Statistical Analysis

Data were expressed as means ± s.e.m. Least-square regression analysis was used to examine the effect of treatment. P values < 0.05 were considered to be significant.

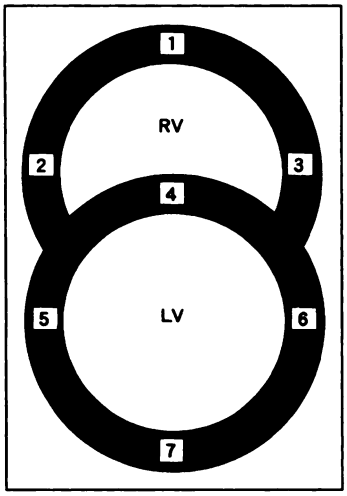

FIGURE 1. Schematic diagram of the right and left ventricles. In the short axial image of the middle ventricular region of the delay image, seven ROI of 6 × 6 pixels were established, including three in the RV free wall, three in the LV free wall and one in the IVS.

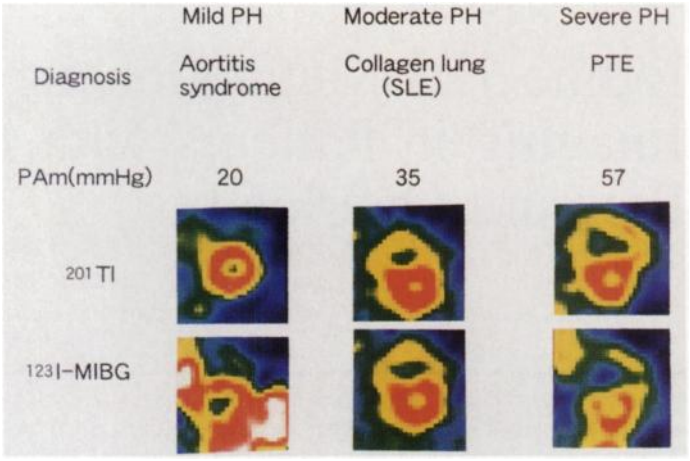

FIGURE 3. Typical [^{123}I]MIBG and ^{201}Tl delayed images. Mild pulmonary hypertension (PH) with mean pulmonary artery pressure (PAm) = 20 mmHg (left), moderate PH (middle) and severe PH (right). Note the morphological changes in each image with increased pulmonary artery pressure.

RESULTS

Figure 3 presents representative examples of short axial ^{201}Tl and [^{123}I]MIBG SPECT (delay image) images at various levels of pulmonary artery pressure. At a mild pulmonary hypertension level (PAm = 20 mmHg), depiction of the right ventricle was very weak, and hypertrophy of the ventricular septum was not observed in either the ^{201}Tl or [^{123}I]MIBG images. At a moderate pulmonary hypertension level (PAm = 35 mmHg), hypertrophy of the right ventricle and ventricular septum and exclusion of the ventricular septum to the left ventricle were observed in the ^{201}Tl and [^{123}I]MIBG images. In severe pulmonary hypertension (PAm = 57 mmHg), hypertrophy and expansion of the right ventricle, hypertrophy of the interventricular septal wall and its incursion into the left ventricle became evident in the ^{201}Tl image. Uptake by the right ventricle and IVS, however, was reduced in the [^{123}I]MIBG image compared with the ^{201}Tl image.

Analysis of the 20 delayed images using the short axial images of the middle ventricular region revealed a significant negative correlation between the IVS-to-LV uptake ratio and the mean pulmonary artery pressure ($r = -0.78$, $p < 0.01$) in [^{123}I]MIBG SPECT. Furthermore, in ^{201}Tl SPECT, the RV-to-LV uptake ratio significantly and positively correlated with the mean pulmonary artery sours ($r = 0.87$, $p < 0.01$) (Fig. 4).

DISCUSSION

Our results demonstrate that the [^{123}I]MIBG images were similar to the ^{201}Tl images at mild to moderate levels of pulmonary hypertension. At severe pulmonary hypertension levels, however, uptake of the [^{123}I]MIBG in the right ventricle and IVS was reduced when compared with ^{201}Tl images. Our

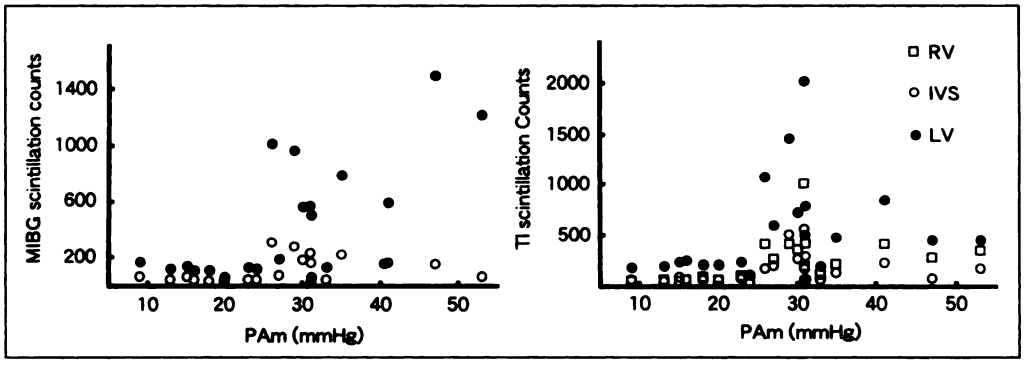

FIGURE 2. Scintillation counts of the IVS and left ventricle (LV) in [^{123}I]MIBG images (left). Scintillation counts of the right ventricle (RV), IVS and LV in ^{201}Tl images (right). RV and LV counts represent the sum of the average counts per ROI, with RV counts = ROI1 + ROI2 + ROI3, IVS counts = ROI4 and LV counts = ROI5 + ROI6 + ROI7.

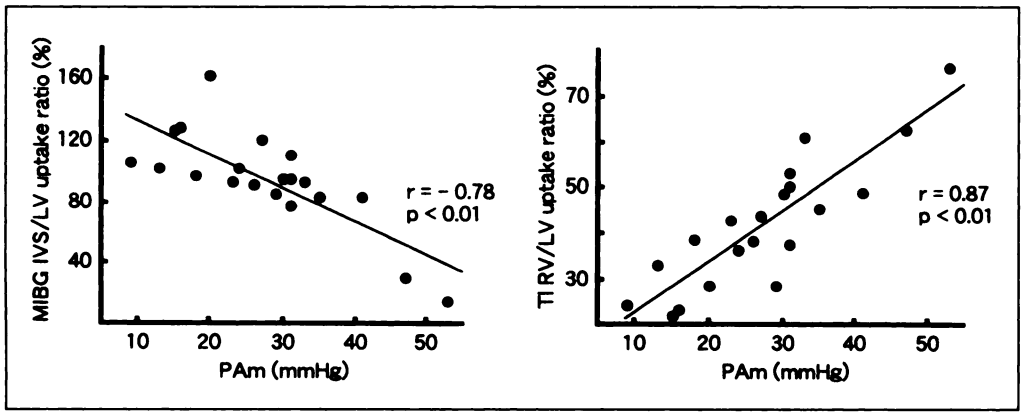

FIGURE 4. Relationship between the IVS-to-LV uptake ratio and mean pulmonary artery pressure (PAm), as determined by [^{123}I]MIBG imaging (left). Note the significant negative correlation between the two variables. Relationship between the RV-to-LV uptake ratio and PAm in ^{201}Tl images, demonstrating a significant positive correlation (right).

results also demonstrate a significant negative correlation between the IVS-to-LV uptake ratio and the mean pulmonary artery pressure observed. On the other hand, hypertrophy of the right ventricle and IVS were observed in ^{201}Tl images as pulmonary hypertension became more severe. These images also revealed incursion of the IVS into the left ventricle and expansion of the right ventricle. Analysis of the same images showed a significant positive correlation between the RV-to-LV uptake ratio and the mean pulmonary artery pressure.

Cohen et al. (*13*) were the first group to analyze the right ventricular free wall in patients with pulmonary hypertension using ^{201}Tl cardiac muscle scintigraphy. Several attempts have been made since then to evaluate right heart load based on depiction levels of the RV free wall of planar images. Several investigators have reported good correlation between the RV-to-LV uptake ratio, determined by ^{201}Tl SPECT, and the systolic pressure of the right ventricle in patients with right ventricular pressure load (*13–15*). Our results agree with these earlier studies in that they demonstrate a good correlation between the RV-to-LV uptake ratio by ^{201}Tl SPECT and the systolic pressure of the right ventricle. Increased mass of the myocardium and oxygen consumption of the cardiac muscle in the chronically-loaded right ventricle may have resulted in increased uptake of ^{201}Tl in the RV wall, which was reflected in the depiction of the right ventricular wall in the images of the cardiac muscle.

Iodine-123-MIBG imaging of the cardiac muscle is usually performed to diagnose diseases of the left heart. To our knowledge, there are no reports on the use of [^{123}I]MIBG imaging to evaluate the clinical conditions associated with right heart loading. Iodine-123-MIBG imaging of the cardiac muscle is used to measure the neuronal and receptor activity of the cardiac sympathetic system. Accumulation of [^{123}I]MIBG involves uptake-1 and uptake-2. Due to the markedly slow clearance of uptake-1, [^{123}I]MIBG concentration remains constant for 4 hr after administration. Due to its rapid clearance, uptake-2 virtually disappears within 4 hr of administration. Therefore, images taken 4 hr postadministration [^{123}I]MIBG, as performed in the present study, correspond to MIBG in storage vesicles, and reflect the norepinephrine content in the sympathetic nerve endings of the cardiac muscle. There is no widely accepted view of myocardial [^{123}I]MIBG distribution in normal, healthy individuals. Due to reduced [^{123}I]MIBG accumulations in the right ventricles of patients with mild or severe pulmonary hypertension, it was difficult to select a small number of ROIs at appropriate sites. To minimize technical errors in measurement and to obtain reliable radioactivity counts in the myocardial wall, we used seven ROIs, each composed of 6 × 6 pixels, on each SPECT image. The radioactivity counts in the RV myocardial wall on [^{123}I]MIBG images were not used for quantitative evaluation.

It has previously been reported, using [^{123}I]MIBG and ^{11}C-CGP-12177 (*16*), that accumulation of [^{123}I]MIBG in the cardiac muscle correlates significantly with the density of beta-adrenoceptors in the incompetent heart (*17,18*). The use of similar imaging techniques, moreover, has recently revealed that down regulation of beta-adrenoceptors reduces accumulation of [^{123}I]MIBG in heart failure (*18,19*). Furthermore, Yoshie et al. (*20*) reported that the density of beta-adrenoceptors in the right ventricle and IVS diminished as monocrotaline-induced RV hypertrophy in rats with pulmonary hypertension progressed. Our study extends these early findings and demonstrates a reduction of [^{123}I]MIBG uptake in the right ventricle and the IVS as hypertrophy of the right ventricle progressed in our patients. A significant correlation was also noted between the mean pulmonary artery pressure and the IVS-to-LV uptake ratio. Our results suggest that impairment of cardiac sympathetic neuronal function of the right ventricle and the IVS occurred in our patients as a result of beta-adrenoceptors reduced density in these regions.

The results of the present study suggest that myocardial SPECT with [^{123}I]MIBG allows noninvasive clinical evaluation of the cardiac sympathetic nerve function in patients with RV pressure overload. Such evaluation has not been possible with any other conventional myocardial imaging technique. When ^{201}Tl myocardial SPECT is used in patients with mild pulmonary hypertension, clear images of the RV free wall are difficult to obtain and ROIs are often difficult to select. By contrast, [^{123}I]MIBG myocardial imaging is simple and allows an accurate evaluation of the severity of RV pressure overload. This is achieved by designating ROIs in the left heart (i.e., in the IVS and LV free wall), without the need to designate ROIs in the RV free wall. This technique is promising for the clinical evaluation of the severity of pulmonary hypertension and its response to treatment.

CONCLUSION

The present study demonstrates that the uptake ratio of [^{123}I]MIBG in the IVS is a useful index for evaluating the severity of pulmonary hypertension, and that chronic RV pressure overload contributes to disturbances of the cardiac sympathetic nervous system.

REFERENCES

1. Sisson JC, Shapiro B, Meyers L, et al. Metaiodobenzylguanidine to map scintigraphically the adrenergic nervous system in man. *J Nucl Med* 1987;28:1625–1636.
2. Sisson JC, Lynch JJ, Johnson LL, et al. Scintigraphic detection of regional disruption of adrenergic neuron in the heart. *Am Heart J* 1988;116:67–76.
3. Sisson JC, Wieland DM, Sherman P, et al. Metaiodobenzylguanidine as an index of the adrenergic nervous system integrity and function. *J Nucl Med* 1987;28:1620–1624.

4. Tobes MC, Jaques S, Wieland DM, et al. Effect of uptake-one inhibitors on the uptake of norepinephrine and metaiodobenzylguanidine. *J Nucl Med* 1985;26:897–907.
5. Nakajyo M, Shimabukuro K, Yosimura, et al. Iodine-131-metaiodobenzylguanidine intra- and extra-vesicular accumulation in the rat heart. *J Nucl Med* 1986;27:84–89.
6. Jaques S, Tobes MC. Comparison of the secretory mechanisms of metaiodobenzylguanidine and norepinephrine from cultured bovine adrenomedullary cells [Abstract]. *J Nucl Med* 1985;25(suppl):17.
7. Fagret D, Eric-Wolf J, Vanzetto G, Borrel E. Myocardial uptake of metaiodobenzylguanidine in patients with left ventricular hypertrophy secondary to valvular aortic stenosis. *J Nucl Med* 1993;34:57–60.
8. Rabinovitch MA, Rose CP, Schwab AJ, et al. A method of dynamic analysis of iodine-123-metaiodobenzylguanidine scintigrams in cardiac mechanical overload hypertrophy and failure. *J Nucl Med* 1993;34:589–600.
9. Merlet P, Valette H, Dubois-Rande, et al. Prognostic value of cardiac metaiodobenzylguanidine imaging in patients with heart failure. *J Nucl Med* 1992;33:471–477.
10. Stanton M, Tuli M, Radtke N, et al. Regional sympathetic denervation after myocardial infarction in humans detected noninvasively using ^{123}I-MIBG. *J Am Coll Cardiol* 1989;14:1519–1526.
11. Abe N, Kashiwagi A, Shigeta Y. Usefulness of ^{125}I-metaiodobenzylguanidine uptake for evaluation of cardiac sympathetic nerve abnormalities in diabetic rats. *J Jpn Diab Soc* 1992;35:113–120.
12. Mantysaari M, Kuikka J, Mustonen J, et al. Noninvasive detection of cardiac sympathetic nervous dysfunction in diabetic patients using ^{123}I-metaiodobenzylguanidine. *Diabetes* 1992;41:1069–1075.
13. Cohen HA, Baird MG, Rouleau JR, et al. Thallium-201 myocardial imaging in patients with pulmonary hypertension. *Circulation* 1976;54:790–795.
14. Ohsuzu F, Handa S, Kondo M, et al. Thallium-201 myocardial imaging to evaluate right ventricular overloading. *Circulation* 1980;61:620–625.
15. Weitzenblum E, Moyses B, Dickele MC, Methlin G. Detection of right ventricular pressure overloading by thallium-201 myocardial scintigraphy. *Chest* 1984;85:164–169.
16. Merlet P, Delforge J, Syrota A, et al. PET with ^{11}C-CGP-12177 to assess beta-adrenergic receptor concentration in idiopathic dilated cardiomyopathy. *Circulation* 1993;87:1169–1178.
17. Delforge J, Syrota A, Lancon TP, et al. Cardiac beta-adrenergic receptor density measured in vivo using PET ^{11}C-CGP-12177 and a new graphical method. *J Nucl Med* 1991;32:739–748.
18. Raum WJ, Laks MM, Garner D, Swerdloff RS. Beta-adrenergic receptor and cyclic AMP alterations in the canine ventricular septum during long-term norepinephrine infusion: implications for hypertrophic cardiomyopathy. *Circulation* 1983;68:693–699.
19. Fowler MB, Laser JA, Hopkins GL, Minobe W, Bristow MR. Assessment of the beta-adrenergic receptor pathway in the intact failing human heart: progressive receptor down regulation and subsensitivity to agonist response. *Circulation* 1986;74:1290–1302.
20. Yoshie H, Tobise K, Onodera S. Intraventricular changes in the beta-adrenoceptor adenylate cyclase system of monocrotaline induced right ventricular hypertrophy. *Jpn Circ J* 1994;58:855–865.

Renal Technetium-99m-DMSA SPECT in Normal Volunteers

C. De Sadeleer, A. Bossuyt, E. Goes and A. Piepsz
Departments of Nuclear Medicine, Radiology and Pediatrics, AZ-VUB, Brussels, Belgium

Dimercaptosuccinic acid (DMSA) renal scintigraphy today is considered a sensitive and useful technique for the detection of cortical abnormalities. Recent studies have suggested that lesion detection can be improved by SPECT imaging. This study investigated normal kidneys using different SPECT modalities. **Methods:** Ten young, healthy volunteers with normal clinical history and normal renal ultrasound underwent planar and SPECT DMSA imaging 2 to 4 hr after intravenous injection of ^{99m}Tc-DMSA (185 MBq). Analysis of SPECT data was focused on the homogeneity of cortical uptake (comparison of upper and lower pole activity) as well as on the presence or absence of focal cortical defects. **Results:** No abnormality could be observed on the planar images. SPECT revealed, in seven kidneys (five left and two right), the presence of a hypoactive upper pole. This was visually observed on the coronal slices with up to 35% difference between upper and lower pole. Moreover, three focal cortical defects were visualized on the coronal slices as well as on three-dimensional surface shade displays. **Conclusion:** These normal patterns should be recognized when evaluating a patient with possible renal involvement.

Key Words: renal imaging; technetium-99m-DMSA; SPECT
J Nucl Med 1996; 37:1346–1349

The ^{99m}Tc-dimercaptosuccinic acid (DMSA) renal scan is now widely recognized as a reference method for the evaluation of renal parenchymal disease. The traditional planar technique provides adequate two-dimensional imaging of the renal cortex and most of the validation studies that have defined the clinical value of DMSA scintigraphy were obtained by these conventional planar imaging techniques.

The introduction of high-resolution SPECT offers the opportunity to image the kidneys with even more precise cortical detail. State-of-the-art SPECT not only has a spatial resolution of less than 1 cm, but image contrast is also dramatically improved in the tomographic slices.

Recent reports suggest a higher sensitivity of SPECT compared to planar imaging. However, because of normal variations in kidney anatomy, any increase in contrast obtained by SPECT imaging also creates opportunities for false-positive interpretation.

To evaluate the potential importance of that problem, and to obtain a dataset of normal SPECT images, we compared the results of conventional planar DMSA scintigraphy with those of SPECT using standard and reoriented coronal, sagittal and transverse slices, as well as three-dimensional total organ surface shade images, in a group of normal healthy volunteers.

MATERIAL AND METHODS

Ten healthy volunteers (5 men, 5 women; mean age 23 yr; range 19.7–25.8 yr) were enrolled in this study. They had no history of previous urinary tract disease, fever of unknown origin, hypertension or abdominal trauma. Physical examination, including blood pressure, was normal. Before entering in the study all volunteers underwent an ultrasonographic study of the kidneys in order to exclude any pelvic and calyx distention, renal surface abnormality, expansive masses, tissue texture change or abnormal renal size.

Both planar and SPECT studies were acquired 2 to 4 hr after intravenous injection of 5 mCi (185 MBq) ^{99m}Tc-DMSA. The order of imaging was random.

Planar Imaging

Planar images were obtained with a standard gamma camera equipped with a high-resolution, low-energy collimator, from posteriorly, with the patient in the supine position, and from both posterior oblique sides. Data were acquired in a 256 × 256 matrix, word mode, 300,000 counts per view. No zoom or pinhole images were performed.

Received July 21, 1995; revision accepted Oct. 20, 1995.
For correspondence or reprints contact: Carlos De Sadeleer, MD, A.Z. V.U.B., Department of Nuclear Medicine, Laarbeeklaan 101, 1090 Brussels, Belgium.